

# A NOVEL LOW-LIGHT-LEVEL OPTICAL SWITCH BY USING NANO-OPTO-MECHANICS TECHNOLOGY

Jifang Tao, Hong Cai, Lennon Yao Ting Lee, and Yuandong Gu

Institute of Microelectronics, A\*STAR (Agency for Science, Technology and Research)  
2 Fusionopolis Way, #08-02 Innovis Tower, Singapore 138634

## ABSTRACT

An all-optical switch that controls a strong light with a weak one based on nonlinear cavity enhanced optomechanical effect is demonstrated. It consists of a micro-ring resonator with suspension arcs, and a bus waveguide. “On” and “off” states of the probe light depend on the position of the suspension arcs that is under the control by a weak signal light. By use of nano-opto-mechanics system (NOMS) technology, the device is fabricated on silicon photonics platform with a foot-print size of only  $50\text{ }\mu\text{m} \times 50\text{ }\mu\text{m}$ . The switch is studied through both modeling and experiment. The observed control light is 380 times smaller in intensity than the probe light. Potential applications of this switch include quantum information networks, optical memories, on-chip optical signal processing, etc.

## INTRODUCTION AND DESIGN

An all-optical switch is a photonic device in which one light beam is controlled by another one. It is one of the most fundamental elements to construct an all-optical high speed information network and computing system [1-4]. Many solutions have been demonstrated in a wide variety of materials, including those based on the intensity-dependent refractive index or saturable absorption of transparent nonlinear optical materials [5-6, 8]. However, the control light intensity must be much higher than probe light because of the relatively weak non-linear optics effect in most of optical materials. Slow light and cold atoms can be used to enhance nonlinear effects but they are not practical for most applications due to the limitation of cost and size [7]. Other approaches are based on the instability of transverse optical patterns that are generated when the laser beams counter-propagate through an atomic vapor, such as warm rubidium vapor, the systems need many separate optics components and are difficult to reduce the size of the bulky functional system down to chip-scale device [9-11].

Except nonlinear optical medium based all-optical switch, the optomechanics effect in NOMS devices provides an alternative solution to realize all-optical control [12-13]. Here we demonstrate a novel NOMS device to release all-optical switch working at low-light level. Figure 1(a) shows a basic see-saw balance system. The strong light (probe) generates a strong gradient optical force via a suspended photonic structure. The optical force is balanced by the mechanical restoring force at the initial state. When a tiny force (control light) appears, this balance is broken immediately. Based on this mechanism, the “on” and “off” states of the strong probe light can be controlled effectively by a weak control light. Figure 1(b) show the schematic of the device that proves the concept of the see-saw mechanism. The device consists of a partially suspended micro-ring resonator and

a bus waveguide. Both probe light and control light are injected into the device via the bus waveguide. A strong optical gradient force is excited by the probe light loading on the suspended part of the micro-ring resonator, which bends the suspension part of the waveguide down to substrate. It will be automatically balanced when the mechanical resorting force equates to optical gradient force.

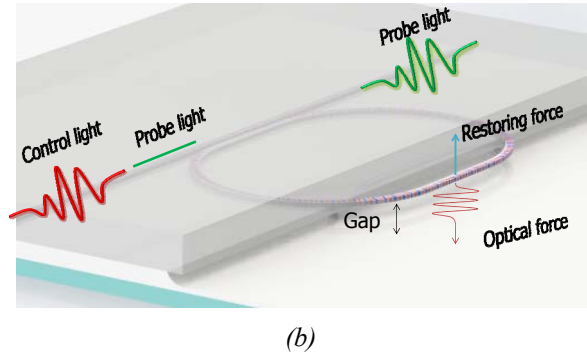
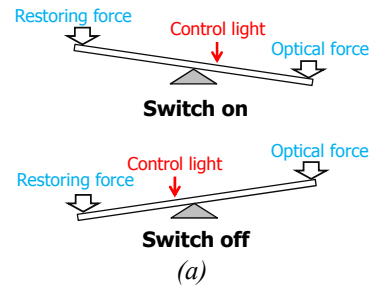


Figure 1: Schematic of the all-optical switch working at low-light level. (a) Generic optomechanical system working as a see-saw. A weak control light is enough to control the states of the see-saw. (b) Schematic of the all-optical switch consists of a micro-ring resonator with a suspension arc. The “on” and “off” states of the switch is controlled by the states of the suspension arc balanced by the optical gradient force and the mechanical restoring force.

The derivative of the optical energy with respect to the gap gives the gradient optical force. Thus, the optical gradient force strongly depends on the total power in the micro-ring resonator. For the micro-ring resonator, its circulating power ( $P_{ring}$ ) of the resonance is determined as [13]

$$P_{ring} = \frac{\alpha^2(1-|t|^2)}{1+\alpha^2|t|^2-2\alpha|t|\cos(\theta+\varphi_t)} P_{in} \quad (1)$$

where  $P_{in}^2$  is the input optical power,  $\alpha$  is the loss coefficient of the ring,  $|t|$  represents the coupling losses,  $\phi$  is the phase of the coupler, and  $\phi_{rt}$  is the round trip phase which is determined by the wavelength. The magnitude of the optical gradient force (unit:  $pN$ ) not only depends on the optical power in the micro-ring resonator ( $P_{ring}$ ), but also strongly depends on both separation gap ( $g$ ) between the suspended arc and substrate, and the wavelength of the input light ( $\lambda$ ). The optical gradient force can be expressed as [14]

$$F_{opto} = \frac{1}{n_{eff}} \frac{\partial n_{eff}}{\partial g} \frac{P_{ring}(\lambda, g) L n_g}{c} \quad (2)$$

where  $n_{eff}$  is the effective index of the suspended arc of the micro-ring resonator,  $n_g$  is the group index of the mode in the micro-ring,  $L$  is the length of the suspended arc, and  $c$  represents the light speed in vacuum. It should be noted that  $P_{ring}$  is a function of the optical wavelength and the separation gap because of the micro-ring resonator. The micro-ring resonator has resonant modes that allows light of resonant wavelengths to circulate in the ring for a longer period. Furthermore, the resonances can be shifted by the bending of the micro-ring resonator. This explains how the optical power in the optical gradient force is dependent on the wavelength and the separation gap. The optical power can change when the suspended arc bends down. It can increase or decrease based on the offset between resonant condition determined by micro-ring and input light wavelength.

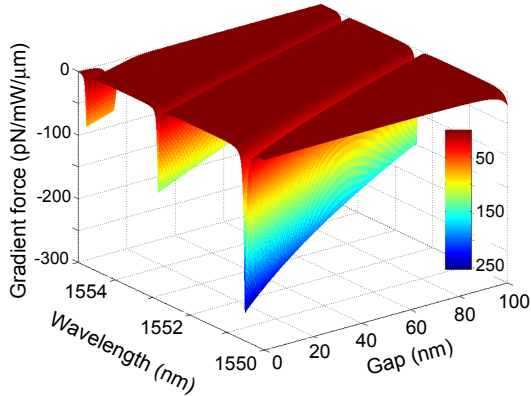


Figure 2: Simulated optical gradient force that is determined by the optical wavelength of the input light and separation gap between arc and substrate. The gradient force is normalized with respect to the length of the suspended arc and the input optical power.

Figure 2 shows the simulation results of the optical gradient force. At the same injection optical power, the optical gradient force can be much different. Light with low power can generate a large optical gradient because it can bend the arc down to a position that the light with high power meets the resonance condition. When the arc deflects, the elasticity of the arc gives rise to a mechanical restoring force [3],

$$F_{mech} = k\Delta g \quad (3)$$

where  $k$  is the spring constant of suspended arc,  $\Delta g$  is the changes of the separation gap. This restoring force tends to pull the arc back to the neutral position. Since the deflection induced by optical gradient force is very small, the mechanical spring constant of the arc can be regarded as a fixed value which can be calculated by the finite element simulation model. These two forces,  $F_{mech}$  and  $F_{opto}$  can quickly balance each other at an equilibrium point.

## EXPERIMENTAL RESULTS

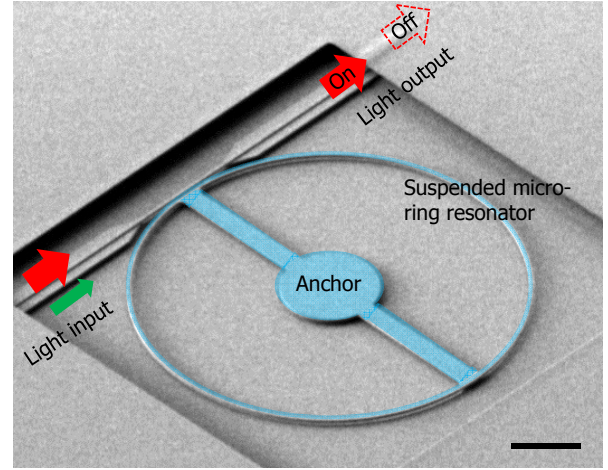


Figure 3: SEM of the fabricated NOMS all-optical switch. Length of the dimension bar is 5  $\mu m$ .

The scanning electron micrograph (SEM) of the all-optical switch is shown in Fig. 3. It was fabricated based on standard SOI wafer with a structure layer of 220 nm, and buried oxide (BOX) layer of 2  $\mu m$ . The device is patterned by deep UV lithography and etched by plasma dry etching. Then, the waveguide is covered by a layer of SiO<sub>2</sub> cladding (around 1.5  $\mu m$ ) deposited by PECVD. To protect unwanted waveguides outside of release window, a thin Al<sub>2</sub>O<sub>3</sub> layer ( $\sim 15$  nm) is deposited by ALD. Finally, part of the BOX layer is removed using HF-vapor with precisely timed control. Similar process has been reported in our previous work [15-16]. The footprint of the switch is around 50  $\mu m \times 50 \mu m$ . The radius of the micro-ring resonator is 15  $\mu m$ , and the width of the waveguides is around 400 nm. Two inversed tips are fabricated to improve the coupling efficiency between the waveguide and lensed-fiber. The tested coupling loss per facet is around 3 dB.

Figure 4 shows the switching of the strong probe light by use of the weak control light. In the experiment, two tunable light sources generate the control light and probe light. In order to detect the changes of the resonances of the micro-ring resonator, a broadband light from an amplified spontaneous emission (ASE) source is also injected into the devices. These three light beams are coupled into the bus waveguide of the device via a nano-alignment system. After normalizing to a straight waveguide, the transmission spectra are shown in Fig. 4. Power of the control light is around -36 dBm which is 380 times lower than the power of the probe light of -10.2 dBm. Figure 4(a) shows the probe light switches from “on” to “off” states. Once the

weak control light appears, the strong probe light can be switched from “on” to “off”. The strong probe light is switched from “off-resonance” state to “on-resonance” state because the suspended arc bends downwards driven by the control light. Figure 4(b) shows the switch state from “off” to “on”, because the probe light is from “on-resonance” state to off-resonance state. Although the weak control light increases the optical gradient force at the beginning, it pulls the suspended arc further downwards till the total energy in the micro-ring resonator drops quickly due to the probe light being “off-resonance”. Finally, the arc bends up and returns its original position in steady state and both the probe light and the control light are not at resonance in the micro-ring resonator. Further work would analyze the damping effects, the effect of the ASE and optimize the system to reduce the switching time.

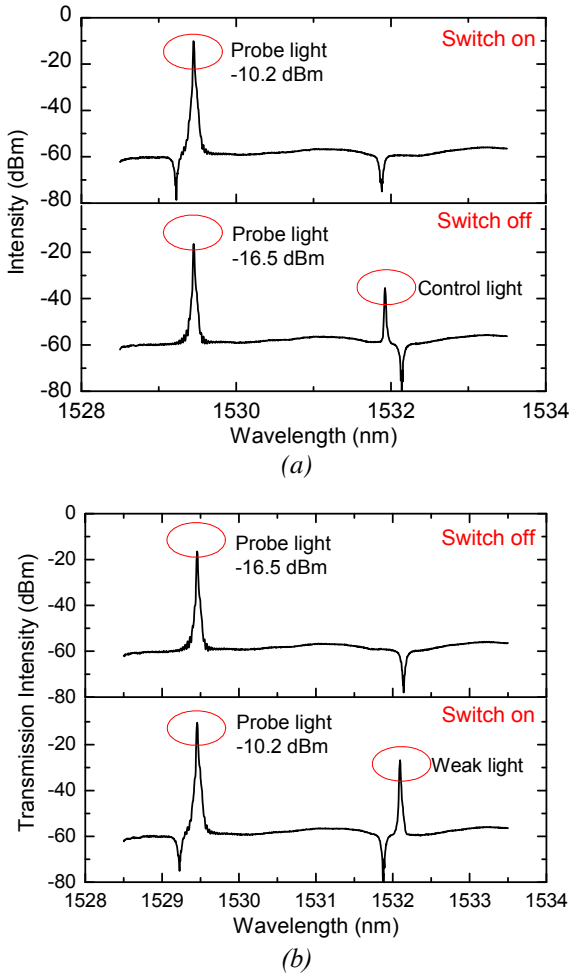


Figure 4: Switches of the probe light from “on” state to “off” when weak control light is injected into the device. Power of the control light is around -36 dBm which is 380 times lower than the power of probe light of -10.2 dBm.

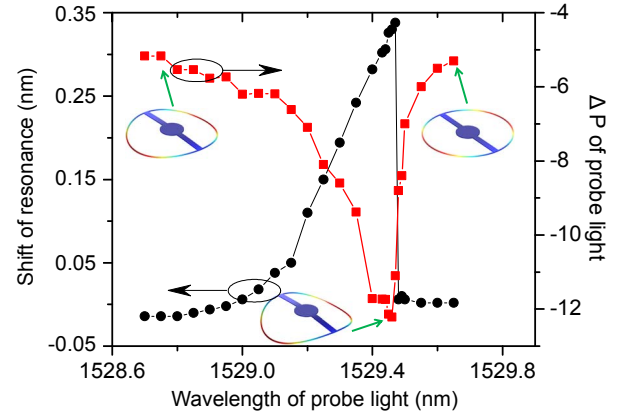


Figure 5: Switching properties of the NOMS switch. The graph shows the relationship between the shift of resonance from the resonator at the “switch on” position and the extinction ratio vs. the wavelength of the probe light.

The extinction ratio (ER) of the all-optical switch can be improved by optimizing the wavelength of the probe light. For a micro-ring resonator with suspension arcs, the resonance red-shifts when the suspension arc bends down. The bending down can be realized by either increasing the optical power or increasing the wavelength of the probe light. The relationship between the resonant wavelength shift and the probe light wavelength is shown by the black line in Figure 5 with -7 dBm input power. The resonance of the micro-ring resonator red-shifts from the resonator at the “switch on” position as the wavelength of the probe light increases till it is 1529.4 nm. As the probe wavelength increases, it shifts nearer to the actual resonance of the bended micro-ring resonator. The maximum shift value is around 0.3 nm, at which point, the probe wavelength is close to the resonance of the bended micro-ring resonator. After that, the bended free-standing arc returns to the initial state, named as “pull-back” [3]. Before “pull-back”, the suspension arc is balanced by the optical gradient force and mechanical restoring force. And at the point close to “pull-back”, the power of the control light can be quite small. When the free-standing arc is bent down by a light beam from a laser diode with center wavelength of  $\lambda_0$  and linewidth of  $\Delta\lambda$ , its resonant wavelength ( $\lambda_r$ ) around  $\lambda_0$  is always longer than the wavelength center of the light beam  $\lambda_0$ . And at the “pull-back” point, the difference between  $\lambda_0$  and  $\lambda_r$  are the smallest. Thus, most of the probe light resonates in the micro-ring resonator and losses in circulating. Thus, when the probe light switches from “on-resonance” to “off-resonance”, the maximum ER can be obtained. The maximum ER is obtained at 1529.46 nm.

## SUMMARY

A NOMS all-optical switch is demonstrated in which the control power is 380 times smaller than the probe light. The principle is studied through both modeling and experiment. It provides an alternative solution for on-chip all-optical switching at low-light level. This NOMS switch has potential applications for all-optical communications and all-optical computing systems.

## ACKNOWLEDGEMENTS

This work is supported by Singapore Building & Construction Authority (BCA) under Grant No. NRF 2014EWT-EIRP004-002

## REFERENCES

- [1] P. W. Keyes, "Power dissipation in information processing," *Science*, vol. 168, pp. 796-801, 1970
- [2] V. V. Campenhout, W. M. J. Green, Y. A. Vlasov, "Design of digital, ultra-broadband electro-optic switch for reconfigurable optical networks-on-chip," *Opt. Express*, vol. 17, no. 26, pp. 23793-23808, 2009
- [3] M. Ren, J. Huang, H. Cai, J. M. Tsai, J. Zhou, Z. Liu, Z. Suo, and A. Q. Liu, "Nano-optomechanical actuator and pull-back instability," *ACS Nano*, vol. 7, no. 2, 1676-1681, 2013
- [4] T. Chu, H. Yamada, S. Ishida, and Y. Arakawa, "Thermo-optic switch based on photonic-crystal line-defect waveguides," *IEEE Photon. Tech. Lett.*, vol. 17, pp. 2083-2085, 2005
- [5] V. R. Almeida, C. A. Barrios, R. R. Panepucci & M. Lipson, "All-optical control of light on a silicon chip," *Nature*, vol. 431, pp. 1081-1084, 2004
- [6] F. Diebel, D. Keykam, M. Boguslawski, P. Rose, C. Denz, and A. S. Desyatnikov, "All-optical switching in optically induced nonlinear waveguide couplers," *Appl. Phys. Lett.*, vol. 104, 26111, 2014
- [7] D. A. Braje, V. Balić, G. Y. Yin, and S. E. Harris, "Low-light-level nonlinear optics with slow light," *Phys. Rev. A.*, vol. 68, 041801-1 – 041801-4, 2003
- [8] Y. Henry Wen, Onur Kuzucu, Taige Hou, Michal Lipson, and Alexander L. Gaeta, "All-optical switching of a single resonance in silicon ring resonators," *Opt. Lett.*, vol. 36, no. 8, 1413-1415, 2011
- [9] A. M. C. Dawes, L. Illing, S. M. Clark, D. J. Gauthier, "All-optical switching in rubidium vapor," *Science*, vol. 308, pp. 672-674, 2005.
- [10] A. M. C. Dawes, D. J. Gauthier, S. Schumacher, N. H. Kwong, R. Binder, A. L. Smirl, "Transverse optical patterns for ultra-low-light-level all-optical switching," *Laser Photon. Rev.*, vol. 4, no. 2, pp. 221-243, 2010
- [11] C. -Y. Wang, Y. -F. Chen, S. -C. Lin, W. -H. Lin, P. -C. Kuan, and I. A. Yu, "Low-light-level all-optical switching," *Opt. Lett.*, vol. 31, no. 15, pp. 2350-2352, 2006
- [12] J. F. Tao, J. Wu, H. Cai, Q. X. Zhang, J. M. Tsai, "A nanomachined optical logic gate driven by gradient optical force," *Appl. Phys. Lett.*, vol. 100, 113104, 2012
- [13] C. Manolatou, M. J. Khan, S. H. Fan, P. R. Villeneuve, H. A. Haus, and J.D. Joannopoulos, "Coupling of modes analysis of resonant channel add-drop filters," *IEEE J. Quan. Electron.*, vol. 35, no. 9, pp. 1322-1331, 1999
- [14] W. H. P. Pernice, M. Li, and H. X. Tang, "Theoretical investigation of the transverse optical force between a silicon nanowire waveguide and a substrate," *Opt. Express*, vol. 17, no. 3, pp. 1806-1816, 2009
- [15] J. F. Tao, H. Cai, Q. X. Zhang, J. M. Tsai, P. Kropelnicki, A. B. Randles, M. Tang, A. Q. Liu, "A novel transducer for photon energy detection via near-field cavity optomechanics," in *Digest Tech. Papers Transducers'13 Conference*, Barcelona, Spain, Jan. 16-20, 2013, pp. 1511-1514
- [16] H. Cai, B. Dong, F. Tao, L. Ding, J. M. Tsai, G. Q. Lo, A. Q. Liu and D. L. Kwong, "A nanoelectromechanical systems optical switch driven by optical gradient force," *Appl. Phys. Lett.*, Vol 102, 023103, 2013

## CONTACT

- \* J. F. Tao, tel: +65 6770 5418; [taojf@ime.a-star.edu.sg](mailto:taojf@ime.a-star.edu.sg);
- \* Y. D. Gu, tel: +65 6770 5915; [guyd@ime.a-star.edu.sg](mailto:guyd@ime.a-star.edu.sg);